

Automatic Detection Approach of Ship using RADARSAT-1 Synthetic Aperture Radar

Chan-Su Yang*

* Ocean Satellite Research Group, Korea Ocean Research & Development Institute(KORDI)
1270 Sa2-dong Sangrokgu Ansan, Seoul, 426-744, Korea

Abstract : Ship detection from satellite remote sensing is a crucial application for global monitoring for the purpose of protecting the marine environment and ensuring marine security. It permits to monitor sea traffic including fisheries, and to associate ships with oil discharge. An automatic ship detection approach for RADARSAT Fine Synthetic Aperture Radar (SAR) image is described and assessed using in situ ship validation information collected during field experiments conducted on August 6, 2004. Ship detection algorithms developed here consist of five stages: calibration, land masking, prescreening, point positioning, and discrimination. The fine image was acquired of Ulsan Port, located in southeast Korea, and during the acquisition, wind speeds between 0 m/s and 0.4 m/s were reported. The detection approach is applied to anchoring ships in the anchorage area of the port and its results are compared with validation data based on Vessel Traffic Service (VTS) radar. Our analysis for anchoring ships, above 68 m in length (LOA), indicates a 100 % ship detection rate for the RADARSAT single beam mode. It is shown that the ship detection performance of SAR for smaller ships like barge could be higher than the land-based radar. The proposed method is also applied to estimate the ship's dimensions of length and breadth from SAR radar cross section(RCS), but those values were comparatively higher than the actual sizes because of layover and shadow effects of SAR.

Key Words : RADARSAT, Synthetic Aperture Radar (SAR), Ship detection, VTS, Automatic detection approach, RCS

요약 : 인공위성 원격탐사를 이용한 선박탐지는 주요 적용 분야 중 하나로, 광역의 환경 감시와 해상보안에 적용되고 있다. 이를 통하여 어장을 포함한 해상교통을 모니터링할 수 있으며, 기름유출 선박을 찾기도 한다. 본 연구에서는, RADARSAT의 합성개구레이더(SAR) 영상을 기반으로 개발한 자동선박탐지기법을 제시하고, 2004년 8월 6일에 얻어진 영상에 적용을 하여 현장 자료와의 비교를 실시하였다. 선박탐지알고리즘은 보정, 랜드마스킹, 필터링, 위치 등록 그리고 식별의 5단계로 구성된다. 울산항을 중심으로 이루어진 위성 촬영시점의 풍속은 최대 0.4m/s이었다. 전장이 68 m 이상인 묘박지의 선박을 중심으로 한 선박 탐지 결과는 울산 항만교통정보시스템의 레이더정보와 잘 일치하였다. 바지선과 같은 소형 선박의 경우, SAR에 의한 선박 탐지 능력이 육상에 설치된 레이더보다 더 높은 경우도 있었다. 또한, SAR 레이더 산란 단면적(RCS)을 이용하여 선박의 길이와 폭을 계산하였으나, 레이오버와 그림자 효과 때문에 실제 값보다 비교적 높게 추정되었다.

핵심용어 : RADARSAT, 합성개구레이더(SAR), 선박탐지, VTS, 자동탐지기법, RCS

1. Introduction

With the increasing importance in monitoring ship traffic in both coastal and ocean waters, an automatic detection of ships, wakes, and ship velocity is highly desirable. By using land-based radar, Vessel Traffic Service (VTS) has been developed and applied in waterways around the ports. The control of ships near coasts is currently supported by VTS radar but it is restricted because of available information limitations. In addition to that, the coverage of monitoring ships by the traditional VTS is limited to the bay area or the approach from the sea to a harbour. There is a requirement for improving the VTS to be able to

cover areas where radar coverage is almost impossible to achieve.

In 2005, for these reasons, the MARitime Security Service project (MARISS) was started to build, implement and initiate the deployment of a consistent, comprehensive and sustainable portfolio of European Maritime Security Services. MARISS is intended to promote the integration of satellite based maritime surveillance and coastal monitoring with conventional data streams such as AIS, coastal radar, maritime patrol aircraft and intelligence sources for maritime border control and maritime situation awareness.

Yang and Park (2003) suggested an approach merging of satellite remote sensing and environmental stress model to ensure marine safety for the navigational waters off the

* Corresponding Author : yangcs@kordi.re.kr, 031-400-7678

radar range. RADARSAT has the capability to detect both stationary and moving ships on the ocean. Ships are good microwave reflectors, or hard targets, in a sense acting as radar corner reflectors. They return a large portion of the incident energy to the SAR sensor and may appear in the SAR imagery as relatively bright points or elongated bright blobs. Due to this strong hard target behavior, the location of fishing fleets can be easily determined using SAR imagery. Successful SAR detection of ships depends, nevertheless, on the size and type of vessel, the prevailing wind speed conditions, the SAR resolution used and the viewing angle [Vachon et al.(1996; 1997), Morse and Protheroe (1997), Wackerman (1996)]. Yang (2005) proposed an integration of ships information detected from both SAR and VTS.

Previous papers treat methods for detection of ships in SAR image, but are concentrated on a specific step of a full automatic detection system. The detection of ocean features also decreases with high sea states due to higher level of clutter. In this study, pixel coordinates of SAR are converted to UTM and latitude/longitude from SAR platform parameters, and after detecting ship candidates

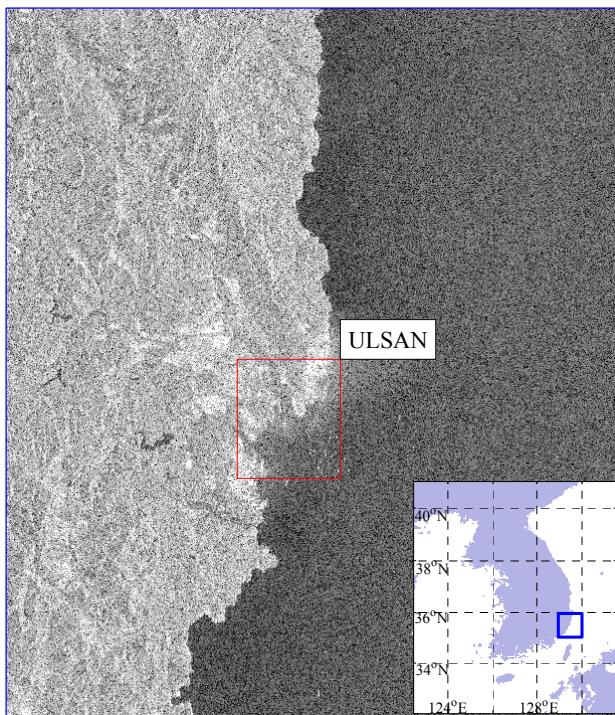


Fig. 1. RADARSAT image, Ulsan Port-centered east coast of south Korea, on August 6, 2004. The image of 17716 lines by 20544 pixels was acquired in F2 mode (incidence angle : 41.2 degrees) and descending passage.

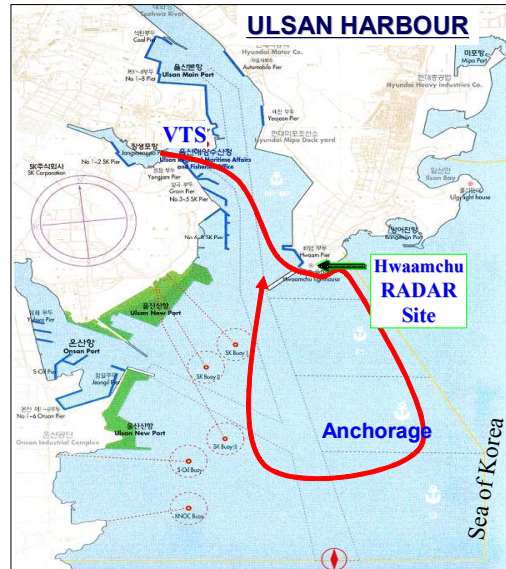


Fig. 2. Map of Ulsan bay. Radar and weather data were measured at Hwaamchu site. The bold line represents a trajectory of ship used here.

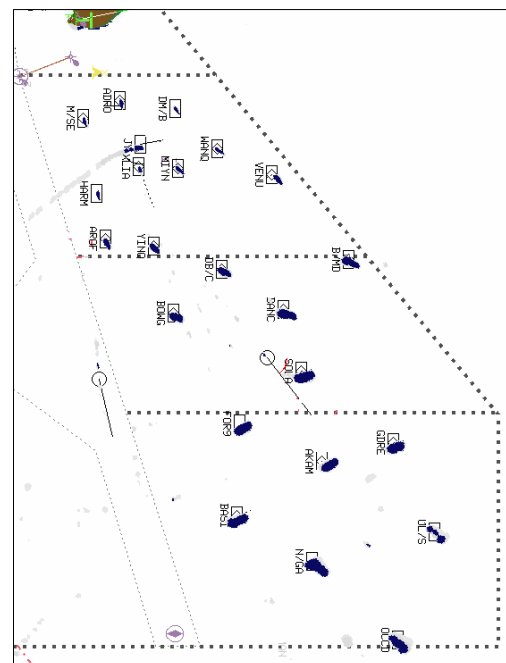


Fig. 3. VTS image at 06:17:49 August 6, 2004 (KST). Ship locations and codes are generated from Radar and AIS data.

ship detection and recognition are tried to decide ship dimension. To minimize the effects caused by sea states, each image is divided into subimages (500 × 500) in which the threshold of ship candidates and the geographical positions are computed.

The work presented in this paper focuses on a

procedure of detecting ship target in a fully automatic way for RADARSAT-1 Fine SAR imagery. The proposed method is to utilize a difference of pixels intensity between ships and sea clutter. Ship detection algorithms consist of five stages: calibration, land masking, prescreening, point positioning, and discrimination including the labeling technique and morphological filtering. The detection examples with RADARSAT-1 SAR are presented, and the ships dimensions are also calculated from the ship images.

2. SAR Data and In-Situ Information

2.1 SAR image data: Fine Mode

RADARSAT-1 satellite SAR data were acquired on August 6, 2004 and processed at the Korea Earth Observation Center (KEOC) as shown in Fig. 1. SAR image is calibrated to geophysical (sigma naught) values of radar cross section (RCS) even if data numbers (DN) on these detected images can be viewed as indicating relative radar backscatter intensities.

2.2 Wind and validation data

During the SAR data acquisition, wind data was acquired from the Hwaamchu station (Fig. 2) and the recorded winds were northwestward, with speeds of 0 m/s ~ 0.4 m/s. The line in Fig. 2 shows a trajectory moved aboard a pilot ship. At the navigation, ship photographs from the scene were taken. The vessels tracked by the Ulsan-VTS during the SAR acquisition are shown in Fig. 3, and listed in Table 1.

Validation data includes the ship name, call sign, latitude/longitude position, ship size and type, and ship photographs from the scene. Automatic Identification System (AIS), a VHF-based self identification system, provides GPS ship positions, and VTS data are used for vessel codes and radar images of ships.

3. Ship Detection Algorithm

3.1 Radar cross section of ships

The ship cross sections are investigated directly from the calibrated image data of each ship types. The example signatures of 3 ship cases are shown in Fig. 4 under F2 mode. In this survey SAR signatures corresponded well to the ship types and were within 7 dB for the ships

Table 1. Ship information : Aug. 6, 2004

Name	Ship Code	LOA (m)	B (m)	Depth (m)	Type
Morning Sea	M/SE	79	14.0	6.7	Chemical T.
Harmony	HARM	68	11.6	5.7	General Cargo
Adoracion	ADRO	78	12.8	5.8	Chemical Gas
Aro Forest	AROF	93	15.8	7.8	Chemical T.
Xin Liang	XLIA	85	16.2	7.2	General Cargo
Ju Yeon	JY	98	15.2	7.5	Petroleum P.
Dongmyung B.	DM/B	73	13.6	7.7	General Cargo
Yinquan	YINQ	105	16.4	7.8	Petroleum P.
Mi Yeon	MIYN	92	14.6	7.4	Petroleum P.
Bow Giovanni	BOWG	127	20.5	10	Chemical T.
Wanquanhai	WANQ	96	15.2	8.4	Petroleum P.
DB Coral	DB/C	111	19.5	10.2	Chemical T.
Venus Gas	VENU	84	15.0	7.0	LPG T.
Formosa Nine	FOR9	167	30.0	14.2	Chemical T.
Basic Arron	BASI	182	32.2	16.5	General Cargo
Danchi	DANC	171	32.0	14.0	Petroleum P.
Solar Oceania	SOLA	162	27.2	13.4	General Cargo
Bunga Melati D.	B/MD	168	30.0	15.0	Petroleum P.
Akama	AKAM	174	32.2	19.1	Petroleum P.
Navios Galaxy	N/GA	216	32.2	19.3	General Cargo
Global Dream	GDRE	154	26.0	11.0	General Cargo
Ocean Concord	OCCD	237	42.0	19.5	Petroleum P.
Ulsan Spirit	UL/S	244	42.7	21.5	Petroleum P.

considered. The maximum RCS come from the bridge area of a ship that causes a double bounce.

Ship detection in SAR amounts to the detection of bright targets against the ocean clutter background. In this experiment, the potential for ship detection depends upon mainly three factors such as the observation geometry, and ship size and type. Most of ship signatures had a regular distribution in a spatial domain, but when the relative angle between ship heading and SAR looking direction is lower than about 30 degrees, its radar echoes were weak and scattered discretely. The scattered signals as in the ship type of petroleum product tanker, therefore, should be grouped in a ship detection processing in order to derive a better detection of ship.

3.2 Ship detection procedure

The proposed scheme of the detection algorithm is illustrated in Fig. 5. The principle of the detection algorithm is based on the theoretical considerations and practical experience, and the algorithm use a processing chain consisting of calibration, land masking, thresholding, point positioning, labeling technique, morphological erosion, morphological dilation, morphological bridging, and attribute-extraction.

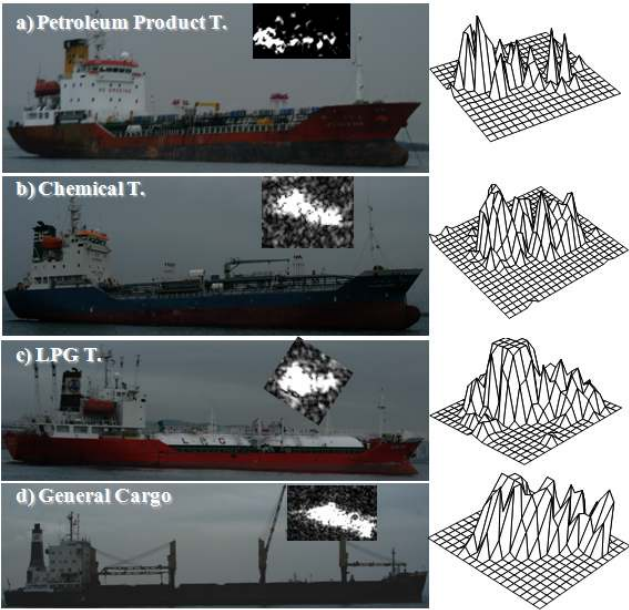


Fig. 4. Ship types, their image intensities (in the image) and mesh plots (right).

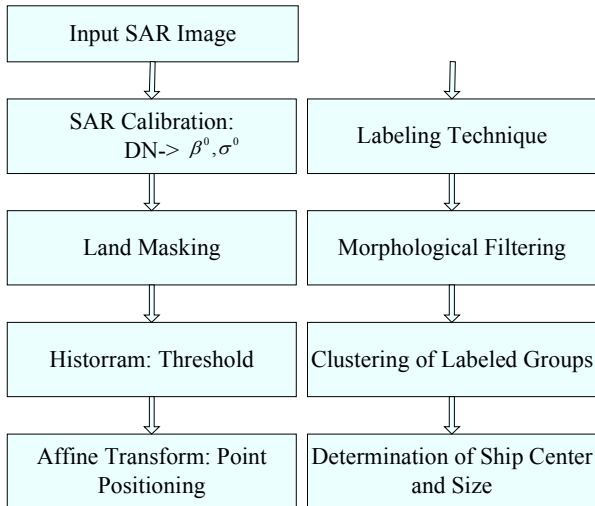


Fig. 5. Flowchart of the proposed algorithm.

After utilizing the Otsu's method [Otsu (1979)] for optimal image thresholding, the input image is converted to grayscale format, and then to binary image by the thresholding. The output binary image has values of 0 (black) for all pixels in the input image with luminance less than the level and 1 (white) for all other pixels. Next connected components specifying 8-connected objects are labeled in the binary image. The pixels labeled 0 are the background. The pixels labeled 1 make up one object, the pixels labeled 2 make up a second object, and so on.

The preregistration is performed using an initial target position that is provided in a header of SAR scene, and an affine transformation is applied to obtain the pixel locations

(longitude and latitude) from the geographic positions of the corners.

Next, it is to find the labeled groups which have more than 10 pixels size, because we also focus on the detection of the relatively large ships such as bulk carrier, container ship, etc. The pixel size threshold in this work varies with the pixel dimension of SAR image.

A morphological filtering is performed to reduce suspicious noise still remaining in the previous step. The combination of the dilation and erosion of morphological filtering is processed to enhance the boundary of the identified ship candidates more clearly. The dilation operation fills the black pixels inside a ship pixel cluster. It also connects the neighboring ship candidate pixels. While dilation adds pixels to the boundaries of objects in an image, erosion removes pixels on object boundaries. The erosion operation also weakens geometric distortion after dilation operation. After the ship candidates are identified approximately, clustering with respect to the distance between central values of the individual pixel groups labeled in the previous work is processed in the whole image to weaken the probability of misidentification of labeled groups using an optimal scale factor. However, there is still a possibility of misidentifying the labeled groups due to unexpected speckle noise. Thus, it is necessary to calculate the minimum of distance between all pixels that belong to the Nth labeled pixel group and all pixels that belong to (N+1)th labeled group. This minimum distance value can refine and re-label pixel groups (ship candidate) which in turn could reduce the likelihood of misidentifying in a fast way. Lastly, the ship center and size are determined from the ship candidates, that are represented by the labeled groups.

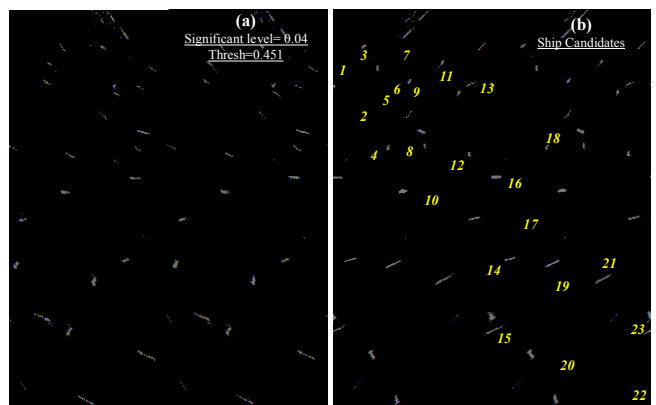


Fig. 6. Ship candidates processed from RADARSAT (left) and 23 vessels in anchorage (right) for comparison with VTS ship list of Table 1. The numbered order represents the list number of Table 1.

Figure 6 (a) shows the labeled groups when the algorithm is applied to the SAR image of Fig. 1, and 23 vessels in anchorage were labeled in numerical order like ship list of Table 1 in Fig. 6 (b).

4. Results

4.1 Validation results with VTS

The validation process is straightforward, requiring comparison of ship validation positions with SAR candidate target positions. As a validation data for RADARSAT Fine Mode, 23 vessels, ranging from 68 to 244 m in length were selected, because their positions show hardly variation with time and are reported to VTS center using AIS. Figure 6 represents the locations of RADARSAT-detected ship targets including 23 vessels in anchorage. Figure 7 is the superposition of the ship targets transmitted by AIS or radar to VTS (PTMS) center and the potential ship targets identified by SAR imagery.

In the comparison it is well shown that the SAR data detected all targets that were reported at VTS. In a portion of ships, a large discrepancy in position appears, but that is

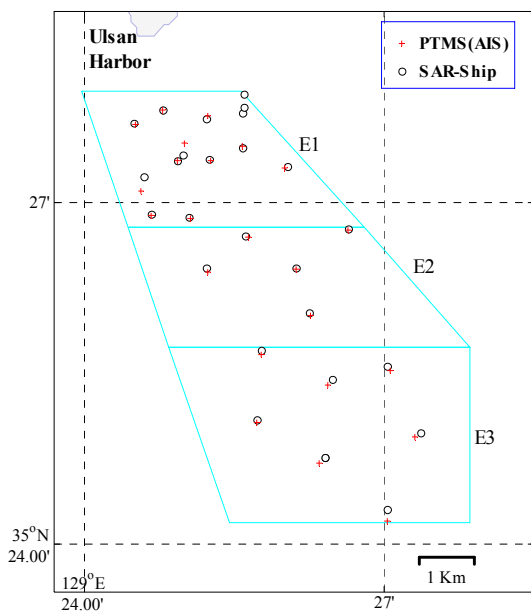


Fig. 7. Collocated RADARSAT and VTS(PTMS) targets.

why the SAR-ship position is calculated as a centroid of potential ship area, and an AIS transmitter is installed on the bridge vicinity of a ship. Overall, the detection rate was 100 %.

Unfortunately, there were very few validation opportunities for smaller vessels. For example, tugboat and

Ship Code	L (m) B (m)	SAR Signature Look Direction	Ship Photo
M/SE	120 43		
ADRO	148 32		
XLLA	115 36		
JY	124 47		
DM/B	81 57		
YINQ	162 28		
MIYN	123 29		
BOW G	146 74		
WAN Q	144 29		
DB/C	145 35		
FOR9	194 51		
BASI	262 54		
DANC	207 53		
SOLA	176 48		
B/M/D	207 41		
AKA M	212 57		
N/GA	292 46		
GDRE	177 39		
OCCD	271 54		
UL/S	266 73		

Fig. 8. Estimation of ship sizes from SAR signatures.

barges in the top-right area of E1 are extracted from the SAR processing, but the coastal radar did not produce any signatures in Fig. 3 because of the shadow zone. As a result, it is shown that the ship detection performance of SAR for smaller ships like barge could be higher than the land-based radar.

4.2 Estimation of ship size

Ship signatures for 20 ship cases with *insitu* photos are listed along with her call signs, lengths and beams in Fig. 8. The proposed method is applied to estimate the ship's dimensions of length and breadth from SAR RCS, but those values were comparatively higher than the actual sizes in Table 1 because of layover and shadow areas. The draft of a ship's hull and large derricks can enlarge a ship size in SAR signatures, and give more effects to a smaller ship. As shown in Fig. 8, the larger a ship size is, the more her overestimation gets.

It is also apparent that ships in length less than 150 m produced different SAR signatures according to the SAR looking direction. As in most cases, when the bridge area of ship was distinguished, the location could be available for the ship heading.

5. Concluding Remarks

In this paper, we introduced a new ship detection technique consisting of the labeling technique, morphological filtering, and Otsu's method. The main advantage of the method is that the difference of intensities between a ship and the sea can be obtained quickly and automatically without human intervention. A disadvantage, however, is that not all pixels detected by this method will be true ship pixels, requiring further processing to be conducted to remove such false pixels.

In this experiment, one fine image of Ulsan Port under calm condition were used to detect stationary ships at anchorage and reveals 100% accuracy for merchant vessels with a variety of types. It is also shown that the ship detection performance of SAR for smaller ships like barge could be higher than the land-based radar. In the estimations of ship length and breadth from SAR RCS, those values were comparatively higher than the actual sizes because of layover and shadow effects.

In the future, sea-ship contrasts that depend on surface wind conditions should be considered to improve this method on a large scale.

Acknowledgement

This work was supported by the Basic Research Project, "Development of Management and Restoration Technologies for Estuaries" of KORDI and the Public Benefit Project of Remote Sensing, "Satellite Remote Sensing for Marine Environment" of Korea Aerospace Research Institute. The author wishes to thank Capt. Jae-Do Lee for his help in arranging a ship.

References

- [1] Morse, A. J. and Protheroe, M. A. (1997), Vessel classification as part of an automated vessel traffic monitoring system using SAR data. *Intl. J. Rem. Sensing*, 18(13), pp. 2709-2712.
- [2] Otsu, N. (1979), A threshold selection method from graylevel histogram, *IEEE Trans. System Man Cybernetics*, Vol. SMC-9, No.1., pp. 62-66.
- [3] Vachon, P., Campbell, J., Bjerkelund, C., Dobson, F., and Rey, M., (1996), Validation of Ship detection by the RADARSAT SAR, *Proceedings PORSEC'96*, Victoria, Canada. pp. 159-169.
- [4] Vachon, P. W., Campbell, J., Bjerkelund, C., Dobson, F., and Rey, M., (1997), Ship Detection by the RADARSAT SAR: Validation of Detection Model Predictions, *Canadian Journal of Remote Sensing*, 23(1), pp. 48-59.
- [5] Wackerman, C. (1996), An algorithm for automatically detecting and characterizing Kelvin wakes in SAR imagery. ERIM Report 606131-1-X, August 1996, Ann Arbor. pp. 248-260.
- [6] Yang, C. S. and Park, Y. S. (2003), Merging of satellite remote sensing and environmental stress model for ensuring marine safety. *Intl. J. Navigation and Port Research*, 27(6), pp. 645-652.
- [7] Yang, C. S. (2005), Vessel Traffic Monitoring Using Spaceborne Synthetic Aperture Radar: An Integrated SAR and VMS, *Ships and Ocean Eng. Tech. Reports*, 39, pp. 65-72.

Received December 10, 2007

Revised 1st : May 25, 2008,

2nd : April 07, 2008

Accepted June 24, 2008